Comparison of Fuel Consumption of Descent Trajectories under Arrival Metering

Tasos Nikoleris[*], Gano B. Chatterji[†]
University of California at Santa Cruz, Moffett Field, CA, 94035-0001

and

Richard A. Coppenbarger[‡]
NASA Ames Research Center, Moffett Field, CA, 94035-0001

This paper compares fuel consumption of descent trajectories from cruise altitude to meter fix when the required time of arrival is later than the nominal time of arrival at the meter fix. The required delay, which is the difference between the nominal and the required times of arrival, is achieved by either slowing down the aircraft in the cruise and descent phases or flying a longer route at a constant altitude. Performance models of ten different Boeing and Airbus aircraft, obtained from the Base of Aircraft Data, are employed for generating the results. It is demonstrated that the most fuel-efficient speed control strategy for absorbing delay is first reducing descent speed as much as possible and then reducing cruise speed. This is a common finding for all ten aircraft considered. For some aircraft, flying at a fixed flight path angle and constant Mach/calibrated-airspeed results in lower fuel consumption compared to standard descent at idle-thrust and constant Mach/calibrated-airspeed. Finally, for the cases examined, it is shown that executing a path stretch maneuver at cruise altitude and descent at a reduced speed is more fuel efficient than inserting an intermediate-altitude cruise segment.

Nomenclature

C_D	=	drag coefficient, dimensionless
C_L	=	lift coefficient, dimensionless
D	=	drag, N
f	=	fuel flow rate, kg/s
g	=	acceleration due to gravity, m/s^2
h	=	altitude, m
L	=	lift, N
M	=	Mach number, dimensionless
m	=	aircraft mass, kg
$\bar{p}$	=	air pressure normalized by sea-level pressure, dimensionless
R	=	specific gas constant for dry air, 287.05287 J / (kg · K)
s	=	ground path distance, m
S_{ref}	=	wing reference area, m^2
T	=	engine thrust, N
V_{CAS}	=	calibrated-airspeed, m/s
V	=	true airspeed, m/s
u_w	=	wind speed along flight direction, m/s
a	=	speed of sound, m/s
γ	=	airmass-relative flight path angle, degrees

---

[*] Associate Research Scientist, University Affiliated Research Center, Mail Stop 210-8, AIAA Member.
[†] Scientist, University Affiliated Research Center, Mail Stop 210-8, AIAA Associate Fellow.
[‡] Aerospace Engineer, Aviation Systems Division, Mail Stop 210-10, AIAA Associate Fellow.

$\bar{\Theta}$	=	temperature normalized by sea-level temperature, dimensionless
κ	=	throttle setting, dimensionless
ρ	=	density of air, kg/m^3
$(\ )_s$	=	sea-level values

I. Introduction

The main requirements for efficient descent under time-based-metering operations in the terminal area are, 1) aircraft remain separated from other aircraft and 2) the required time of arrival constraints at the meter fix be met. Assuming that the aircraft is separated from other traffic along its flight path, a required time of arrival constraint that is later than the aircraft's nominal arrival time can be met using a variety of maneuvers. These include reducing aircraft cruise speed, reducing descent speed, reducing both cruise and descent speeds, slowing down and then descending to a lower altitude, or by cruising for a longer period of time on an extended route. This paper compares the fuel consumption of these strategies for identifying the most fuel-efficient one.

Over the last two decades, a substantial amount of research and development has been done in the United States and Europe to develop decision support tools for controllers to improve safety and efficiency of terminal area operations. A notable example is the Traffic Management Advisor[1] (TMA) that was initially developed at NASA Ames Research Center as one of the Center-TRACON Automation System (CTAS) suite of tools. TMA technology transfer to the Federal Aviation Administration (FAA) led to the development and deployment of the operational version of TMA that is currently used for arrival management at major U.S. airports. TMA computes estimated time of arrival (ETA) to the outer meter arc, meter fix, final approach fix, and runway threshold for each aircraft in the arrival stream[1]. ETAs of the aircraft are used to determine the required times of arrival (RTA) based on sequencing and scheduling constraints. Advisories are then issued by the controller to the pilot to either slowdown or speedup in order to arrive at the control point, such as a meter fix, at the time stipulated by the RTA. The Efficient Descent Advisor[2-4] (EDA), also developed at NASA, generates maneuver advisories that allow controllers to achieve TMA-derived RTA objectives while keeping aircraft separated. EDA provides speed, altitude and heading advisories that can be easily followed by aircraft equipped with a Flight Management System (FMS) to meet an RTA. Depending on the amount of delay, several solutions are possible as discussed in Ref. 2.

Although EDA's solutions have been shown to save fuel in comparison to today's operations in which controllers have no automation for meeting RTAs, research that ranks a broad variety of delay-absorption solutions according to their fuel consumption has been limited. Several studies, such as Refs. 5 through 7, quantified fuel

savings from implementation of continuous descent approaches to an airport. These studies, however, did not seek to determine the most fuel-efficient way for conducting continuous descent to meet an RTA, but only to estimate the benefit of descents without an intermediate cruise segment. Optimum fuel trajectories under a fixed time-of-arrival constraint are examined in Refs 8–9. These studies consider the total energy function of an aircraft without explicit consideration of the typical descent procedure of a commercial airliner, which is transitions from Mach to CAS during descent from cruise altitude to terminal airspace.

The principal contribution of this paper is comparison of fuel efficiency for several standard operational descent procedures with a fixed time-of-arrival constraint at the meter fix, which include a descent segment with constant Mach speed followed by descent at constant CAS. Descent procedures are examined for the two general categories of FMS Vertical Navigation (VNAV) equipage in the field today: 1) performance-based VNAV available on most large commercial transport aircraft, where path guidance is computed based on an idle-thrust assumption in descent, and 2) geometric-path VNAV available on most regional and business jets, where path guidance is based on a fixed flight-path angle relative to the ground. Computation of fuel-optimal trajectories is not the objective of this study; for a thorough study of the problem of determining fuel-optimal delay trajectories the reader is referred to Refs. 8 and 10. This paper considers descent procedures that are typically executed in actual operations, which are not necessarily optimal from a strict fuel consumption perspective. Fuel consumption results in this paper are generated by simulating descent trajectories using Base of Aircraft Data (BADA) version 3.9 (see Ref. 11) performance models of popular Boeing and Airbus aircraft with specified descent procedures such as speed reduction, intermediate altitude, path stretch and fixed flight path angle. Delays ranging from 10 seconds to seven minutes are examined. In all scenarios, the aircraft is initially at cruise altitude and at a distance of 150 nautical miles from the meter fix. Each scenario is characterized by the amount of delay that needs be absorbed and the cruise or descent maneuver used for absorbing that delay. The baseline scenario assumes the aircraft to be cruising at 35,000 feet and wind velocity to be zero. Additional scenarios with different values for cruise altitude and wind conditions are also examined.

The rest of the paper is organized as follows. Section II presents the mathematical model employed for trajectory computation. Descent procedures are discussed in Section III and the nominal descent trajectory is discussed in Section IV. Six different delay absorption strategies that are based on the descent procedures of Section III are described in Section V. Analysis results for the baseline scenario of zero wind and 35,000 feet cruise altitude are

American Institute of Aeronautics and Astronautics

presented and discussed in Section VI. Section VII presents additional results for scenarios where initial cruise altitude and wind conditions vary with respect to the baseline scenario. Finally, Section VIII discusses the conclusions of this research.

II. Aircraft Model

Assuming zero wind, the magnitude of the airmass-relative acceleration resulting from thrust, drag, lift and gravitational forces on the aircraft, modeled as a point-mass, is:

$$\dot{V} = \frac{T - D}{m} - g \sin \gamma \tag{1}$$

where V is airmass-relative speed (true airspeed), T is thrust, D is drag, m is mass, g is acceleration due to gravity, and γ is the flight path angle. The altitude rate is:

$$\dot{h} = V \sin \gamma \tag{2}$$

In the absence of wind, groundspeed is related to true airspeed as follows:

$$\dot{s} = V \cos \gamma \tag{3}$$

With energy defined as $E = h + (1/2g)V^2$, the rate of energy change can be written as $\dot{E} = (T - D)V/mg$ using Eqs. (1) and (2). Trajectory synthesis based on optimal control theory can then be also formulated.[8] In this paper, however, trajectories are generated through use of Eqs. (1)–(3), which more closely emulate typical airline pilot procedures.

A. Drag Model

Aerodynamic drag force is given as the product of the drag coefficient, C_D, and the dynamic pressure as:

$$D = C_D \frac{1}{2} \rho V^2 S_{ref} \tag{4}$$

where ρ is the density of air and S_{ref} is the wing reference area. The drag coefficient is given as the sum of zero-lift drag coefficient, C_{D0}, and the induced drag coefficient, which is a quadratic function of the lift coefficient, C_L. Thus,

$$C_D = C_{D0} + C_{D2}C_L{}^2 \tag{5}$$

Both C_{D0} and C_{D2} are functions of aerodynamic configuration of the aircraft. Traditionally, drag coefficients are given as a function of true airspeed and Reynolds[§] number. BADA models these values as constants for each of the aerodynamic configurations, which are: takeoff, initial climb, clean, approach and landing. BADA provides altitude and speed thresholds for determining these aerodynamic configurations. C_L is obtained using the definition of lift force as:

$$C_L = \frac{2L}{\rho V^2 S_{ref}} \tag{6}$$

Assuming lift equal to weight and small flight path angle,

$$C_L = \frac{2mg}{\rho V^2 S_{ref}} \tag{7}$$

B. Thrust Model

BADA specifies maximum thrust during climb as a quadratic function of altitude. The general expression is:

$$T_{max} = C_{T1}\left(1 - \frac{h}{C_{T2}} + C_{T3}h^2\right) \tag{8}$$

During cruise, thrust is set equal to the drag. A fraction of the maximum thrust is used for idle-thrust descent. It is given as:

$$T_{Idle} = C_{T4} \cdot T_{max} \tag{9}$$

where C_{T1} through C_{T4} are aircraft-specific coefficients.

C. Fuel Flow Model

BADA provides fuel flow models for nominal and idle-thrust conditions. The expression for nominal fuel flow for jet aircraft is given as a function of true airspeed and thrust:

$$f_{nom} = C_{f1}\left(1 + \frac{V}{C_{f2}}\right) \cdot T \tag{10}$$

[§] Reynolds number for a plate of length L is: $Re_L = \rho_\infty V_\infty L / \mu_\infty$, where μ is the absolute viscosity coefficient of the air.

Minimum fuel flow for idle-thrust is:

$$f_{\min} = C_{f3}\left(1 - \frac{h}{C_{f4}}\right) \tag{11}$$

where C_{f1}, C_{f2}, C_{f3} and C_{f4} are aircraft-specific coefficients. Combining Eqs. (10) and (11),

$$f = \max\left(f_{\min}, f_{nom}\right) \tag{12}$$

The amount of fuel consumed, m_f, can be determined by integrating the fuel flow rate f. Thus,

$$m_f = \int_0^\tau f \; dt \tag{13}$$

where τ is the flight time.

III. Descent Procedures

Descent trajectory is divided into a series of flight segments to be consistent with current piloting procedures. Each segment of the descent trajectory shown in Fig. 1 is defined by setting two control variables constant.[12] These variables are: i) engine thrust, ii) speed (Mach or calibrated-airspeed), and iii) altitude rate or flight path angle. Altitude rate is set to zero and Mach or calibrated-airspeed (CAS) is specified in the cruise segment. For constant Mach descent segment, along with the Mach number, either throttle setting κ (equivalent to specifying thrust) or altitude rate $\dot{h}$ or flight path angle γ is specified. If throttle setting is specified, altitude rate and the flight path angle are obtained using Eqs. (1) and (2) as follows. Since

$$\dot{V} = \frac{dV}{dh}\dot{h} \tag{14}$$

$\dot{h}$ can be obtained using Eqs. (1) and (2) as:

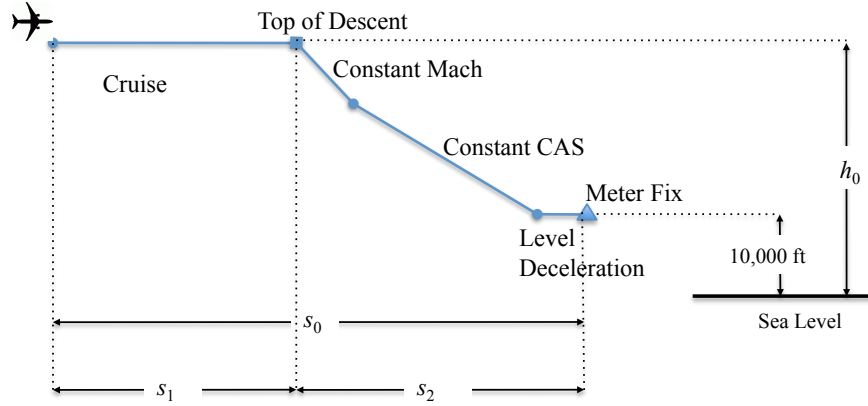$$\dot{h} = \frac{(T-D)V}{mg} \cdot \left(\frac{V}{g}\frac{dV}{dh} + 1\right)^{-1} \tag{15}$$

Figure 1. Vertical profile of aircraft's descent to the meter fix.

The dimensionless quantity $\left(\dfrac{V}{g}\dfrac{dV}{dh} + 1 \right)^{-1}$ is known as the energy share factor; it specifies the proportion of energy allocated to forward motion versus to climb/descent. Share factor is positive during climb, zero during cruise and negative during descent. Since Mach is specified, the derivative of airspeed with respect to altitude can be computed using the standard atmosphere model. Once $\dot{h}$ is computed, γ can be computed using Eq. (2). If altitude rate or flight path angle is specified, Eq. (15) can be used to compute thrust with drag computed using Eq. (4). Constant CAS segment is similar to the constant Mach segment in that a CAS rather than Mach is specified. Along with CAS, either throttle setting or altitude rate or flight path angle is specified. The unknown values are computed using Eq. (15) again because CAS also specifies the derivative of airspeed with respect to altitude via the standard atmosphere model. Finally, in the level deceleration segment, throttle setting is specified and the altitude rate is set to zero. The resulting deceleration is given by Eq. (1). Table 1 lists the controls associated with the segments in Fig. 1.

Table 1. Nominal descent trajectory segments from cruise to meter fix.

Segment type	Controls
Cruise	$\dot{h}=0,\ (M\ \text{or}\ V_{CAS})$
Constant Mach descent	$M,\ \left(\kappa,\ \dot{h},\ \text{or}\ \gamma\right)$
Constant V_{CAS} descent	$V_{CAS},\ \left(\kappa,\ \dot{h},\ \text{or}\ \gamma\right)$
Level deceleration	$\kappa,\ \dot{h}=0$

A. Idle-Thrust Descent at Constant Speed

Idle-thrust descent at constant Mach or CAS is the most frequently employed airline procedure. Pilots set the throttle to idle and maintain a constant Mach until a desired CAS is captured. Beyond that point, descent is maintained at constant CAS. For the constant Mach segment, flight path angle is obtained as

$$\gamma = \sin^{-1}\left\{ \frac{T-D}{m} \cdot \left(M^2 a \frac{da}{dh} + g \right)^{-1} \right\} \tag{16}$$

where a is the speed of sound in air, which is a function of absolute temperature:

$$a = \sqrt{1.4 R \Theta} \tag{17}$$

R is the universal gas constant and Θ is the absolute temperature in degree Kelvin. For the constant CAS segment, flight path angle is obtained using Eq. (15) as:

$$\gamma = \sin^{-1}\left\{ \frac{T-D}{m} \cdot \left(V \frac{dV}{dh} + g \right)^{-1} \right\} \tag{18}$$

where V is related to CAS as follows:

$$V = \sqrt{ 7R\Theta \left(\left\{ \frac{1}{\bar{p}} \left[\left(1 + \frac{V_{CAS}^2}{7R\Theta_s} \right)^{3.5} - 1 \right] + 1 \right\}^{2/7} - 1 \right) } \tag{19}$$

Θ_s is the standard sea level temperature of 288.15 degrees Kelvin. Eq. (19) can be used to determine the term associated with the derivative of true airspeed with respect to altitude required for Eq. (18). It can be shown that:

$$V \frac{dV}{dh} = \frac{7R}{2} \left(\left\{ \frac{1}{\bar{p}} \left[\left(1 + \frac{V_{CAS}^2}{7R\Theta_s} \right)^{3.5} - 1 \right] + 1 \right\}^{\frac{2}{7}} - 1 \right) \frac{d\Theta}{dh} - \frac{R\Theta}{\bar{p}^2} \left\{ \frac{1}{\bar{p}} \left[\left(1 + \frac{V_{CAS}^2}{7R\Theta_s} \right)^{3.5} - 1 \right] + 1 \right\}^{\frac{-5}{7}} \left[\left(1 + \frac{V_{CAS}^2}{7R\Theta_s} \right)^{3.5} - 1 \right] \frac{d\bar{p}}{dh} \tag{20}$$

The right hand side of Eq. (20) can be substituted in Eq. (18) to obtain flight path angle in terms of V_{CAS} and the first derivatives of temperature and normalized air pressure with respect to altitude. Standard atmosphere model provides temperature and pressure as a function of altitude. The altitude rate obtained using the flight path angle in Eq. (2) is integrated forward in time to determine altitude as a function of time.

B. Fixed Flight Path Angle Descent at Constant Speed

An alternative family of descent trajectories can be obtained by keeping the flight path angle and speed (Mach or CAS) constant during descent. This concept is illustrated in Fig. 2. Since flight path angle is kept constant, Eq. (2) can be used to determine the altitude rate, which can be integrated to determine the altitude. Thrust along the constant Mach and CAS segments varies by altitude and is obtained by rearranging Eqs. (16) and (18) as follows:

$$T = D + m\left(M^2 a \frac{da}{dh} + g \right)\sin\gamma \tag{21}$$

and

$$T = D + m\left(V \frac{dV}{dh} + g \right)\sin\gamma \tag{22}$$

where the term associated with the first derivative of airspeed with respect to altitude is given in terms of CAS in Eq. (20). Assuming speed brakes are not used, the thrust values obtained from Eqs. (21) and (22) should not be smaller than idle-thrust computed using Eq. (9). Speed needs to be increased if this happens, to comply with the idle-thrust constraint.
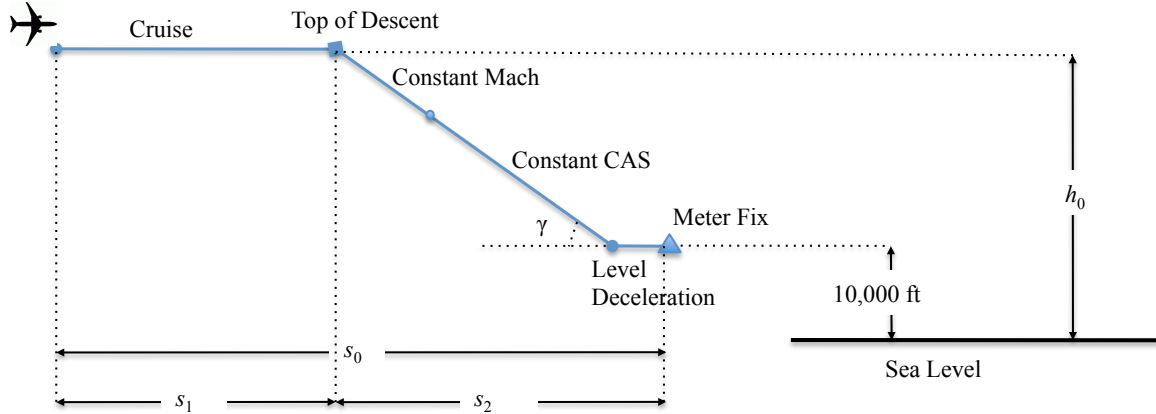

Figure 2. Descent at constant speed and fixed flight path angle.

C. Level Flight

For level deceleration, throttle is set to idle and Eq. (1) is integrated to obtain true airspeed, which is then used to compute drag via Eq. (4). Thrust is set equal to drag for cruise at constant speed.

IV. Nominal Trajectory

The nominal scenario employed in this study is as follows. The meter fix is assumed to be located at the TRACON boundary at an altitude of 10,000 feet. The aircraft is assumed to be at the TMA freeze horizon, a distance s_0 from the meter fix, and at cruise altitude h_0 above mean sea level at time t_0. TMA stops updating the RTA of the aircraft when the aircraft is about 19 minutes away from the meter fix. This roughly translates to a TMA freeze horizon of 150 nautical miles (nmi). Cruise altitude is assumed to be 35,000 feet, which is a typical cruise altitude of commercial jets. Aircraft is constrained to cross the meter fix at a CAS of 250 knots or less. Figure 3 illustrates the corresponding vertical trajectory.
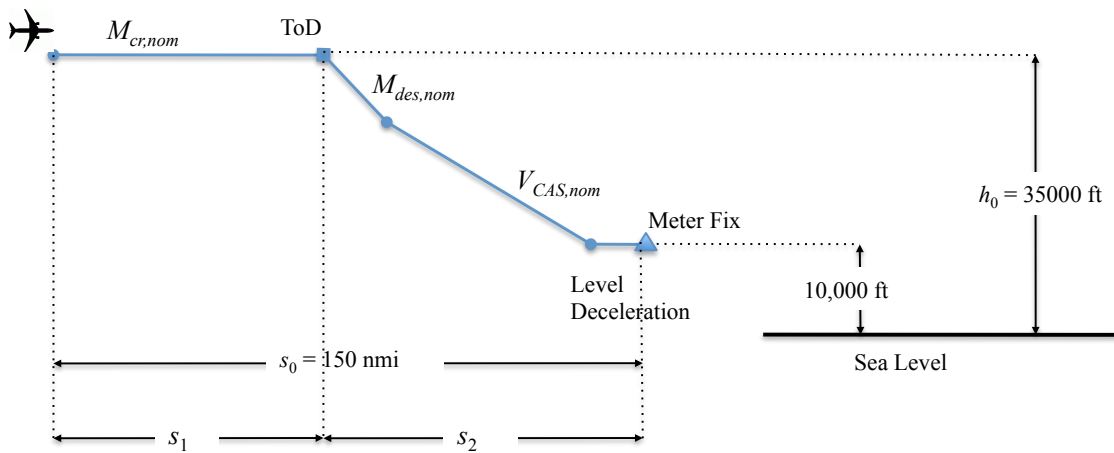
Figure 3. Vertical profile of aircraft's nominal trajectory to meter fix.

The vertical trajectory shown in Fig. 3 is broken into constant Mach, constant CAS and level deceleration segments. Speed values needed for these segments for different aircraft are available in BADA. Consistent with actual pilot procedures,[7,13] the *nominal* trajectory is specified by the following flight segments:

a. Cruise at 35,000 ft at nominal Mach, $M_{cr,nom}$, until the Top–of–Descent (ToD) point.

b. Idle-thrust, constant Mach descent at $M_{des,nom}$ until CAS becomes equal to $V_{CAS,nom}$. If $M_{cr,nom} < M_{des,nom}$, idle-thrust descent at fixed flight path angle until $M_{des,nom}$ is captured. Descent rate of 1,100 ft per 3 nmi used in this case. If $M_{cr,nom} > M_{des,nom}$, level deceleration to $M_{des,nom}$ prior to ToD.

c. Idle-thrust, constant CAS descent at $V_{CAS,nom}$ till meter fix altitude of 10,000 ft.

American Institute of Aeronautics and Astronautics

d. Level deceleration from $V_{CAS,nom}$ to CAS of 250 knots.

The vertical trajectory consisting of segments (b) through (d), discussed above, is determined using the procedures discussed in Section III. An output of this process is the horizontal trajectory (s,t), which enables computation of s_2. Location of ToD point at the end of the cruise segment, s_1, is obtained by subtracting s_2 from s_0. Fuel consumption of each aircraft's nominal trajectory is defined as *baseline* fuel burn.

The time at which the aircraft is expected to arrive at the meter fix flying its nominal trajectory from the freeze horizon is defined as the Estimated Time of Arrival (ETA). Similarly, the time at which the aircraft is scheduled to arrive at the meter fix by TMA is denoted as the Required Time of Arrival (RTA). The difference between RTA and ETA is defined as the delay that needs to be absorbed along the cruise and descent segments. Delays of 10 seconds to 7 minutes have been considered in this study based on the range of delays typically assigned by TMA.

Along with available cruise distance before the ToD point, s_1, another parameter that affects the amount of delay that can be absorbed is aircraft's minimum speed. Minimum speed is stipulated to be 30% above the stall speed (see Ref. 10); it is a function of altitude, and aircraft's aerodynamic configuration and weight. Minimum speed decreases with decreasing weight. In practice, higher minimum speeds are assigned by Air Traffic Control (ATC) for safety. For cruise at high altitude, ATC typically does not assign speeds below Mach 0.71 and CAS below 250 knots. ATC also does not assign speeds above the maximum Mach and CAS limits specified in the aircraft's flight envelope. Figure 4 shows the flight envelope of a jet aircraft. The two thick lines mark the lower stall limit and the upper structural limit. This figure also shows examples of a fast and a slow trajectory, labeled "Case 1" and "Case 2" respectively, starting at 35,000 feet altitude and terminating at 10,000 feet altitude. The fast trajectory, Case 1, consists of descent at constant Mach to about 28,000 feet altitude, which is the Mach transition altitude, followed by constant CAS descent at about 310 knots to 10,000 feet altitude and then deceleration to 250 knots. The slow trajectory, Case 2, consists of deceleration at cruise altitude to about Mach 0.74 and then descent at CAS of 250 knots.
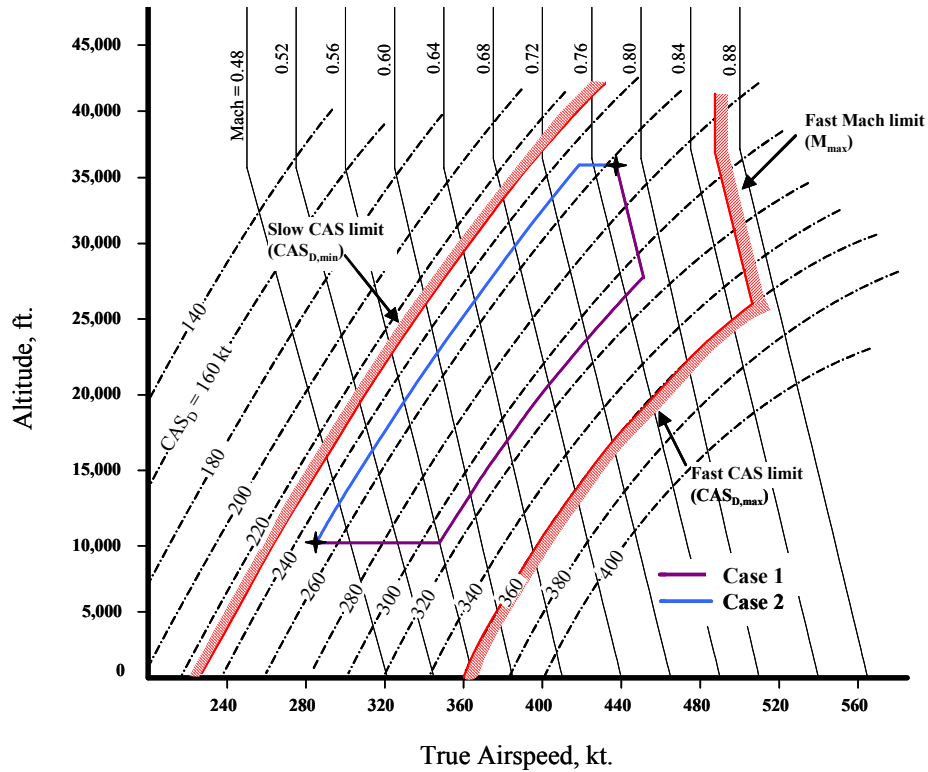
Figure 4. Example of a typical flight envelope for a jet-engine aircraft. (source: Ref. 2)

V. Delay Absorption Strategies

Strategies for absorbing delay to meet RTA at the meter fix can be grouped into two categories. The first category consists of strategies that only use speed adjustments. The second category consists of strategies that change speed and also modify vertical or horizontal trajectory. The following four strategies belonging to the first category are considered: 1) reduce only cruise Mach, 2) reduce only descent CAS, 3) reduce cruise Mach followed by descent CAS and 4) reduce descent CAS first and then reduce cruise Mach. These commonly employed airline strategies are conducted at constant Mach and CAS. For large jet transports equipped with a performance-based FMS, the descent portion is typically conducted at idle-thrust. For regional and business jets equipped with an FMS that uses geometric vertical path guidance, the descent portion is typically conducted at non-idle thrust along a fixed flight-path angle.[14] From the second category, the strategies of path stretch and intermediate cruise segment are analyzed. Table 2 summarizes all six delay absorption strategies.

Table 2. Delay absorption strategy descriptions.

Strategy	Description
Cruise-only	Reduce only cruise Mach speed, with M_{min} as lower limit.
Descent-only	Reduce only descent CAS, with 250 knots as lower limit.
Cruise-first	Reduce cruise Mach first as much possible, and then reduce descent CAS to absorb remaining delay.
Descent-first	Reduce descent CAS first as much possible, and then reduce cruise Mach to absorb remaining delay.
Path stretch	Reduce cruise Mach to M_{min} and then execute path stretch to absorb remaining delay.
Intermediate Cruise Segment	Descent at minimum CAS and execute intermediate cruise segments at M_{min} to absorb remaining delay.

A. Cruise-only Strategy

Slowing down aircraft in the cruise phase is frequently used to absorb up to one and a half minutes of delay. Instead of cruising at the nominal Mach, $M_{cr,nom}$, the aircraft is slowed down to Mach of M'_{cr} to arrive later. The minimum Mach, $M_{cr,min}$, was set to 0.71 for large jets and 0.74 for heavy jets based on discussions with air traffic controllers. After the ToD point, Mach of M'_{cr} is maintained during descent at idle-thrust (or constant γ) until the CAS becomes equal to the nominal CAS, $V_{CAS,nom}$. This CAS is maintained till meter fix altitude. Then, the aircraft is decelerated to a CAS of 250 knots. Figure 5 illustrates the associated vertical trajectory segments.

To find M'_{cr}, cruise Mach is reduced in increments of 0.01 starting from $M_{cr,nom}$ with $M_{cr,min}$ as the lower bound. Aircraft trajectory and the resulting time of arrival at the meter fix are computed for each value. Computations are halted when the time of arrival at the meter fix is within $\pm 5\,\mathrm{s}$ with respect to the RTA.
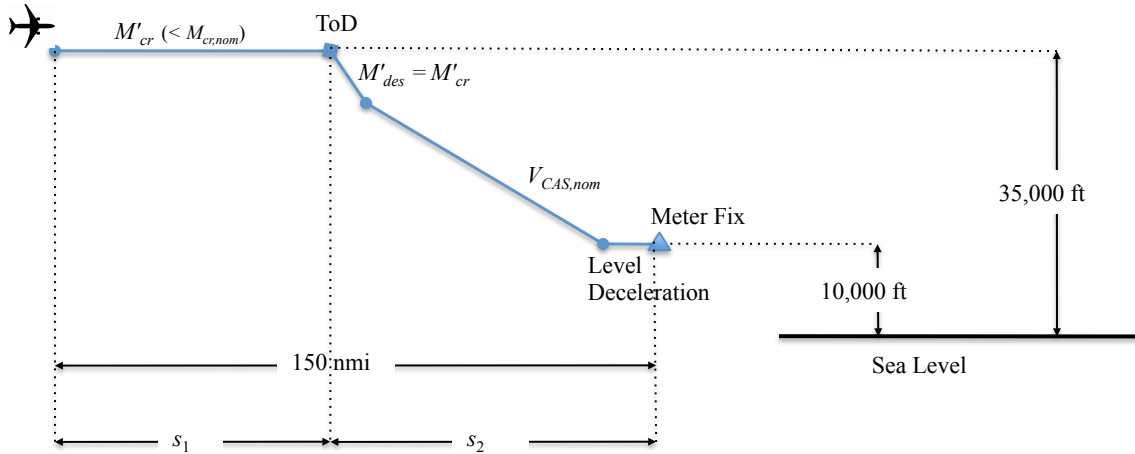
Figure 5. Vertical trajectory profile for the cruise-only strategy.

B. Descent-only Strategy

Aircraft cruises at the nominal Mach. This Mach is maintained during idle-thrust (or constant γ) descent until a CAS of V'_{CAS} is attained, which is less than $V_{CAS,nom}$. Starting from $V_{CAS,nom}$, CAS is reduced in increments of one-knot for computing the trajectory and the time of arrival at the meter fix. The minimum value of V'_{CAS} is set to 250 knots, which is generally the minimum CAS that can be assigned to aircraft flying above 10,000 feet by air traffic controllers. The algorithm terminates when the time of arrival at the meter fix is within $\pm\,5\,\text{s}$ with respect to the RTA. Figure 6 illustrates the conceptual trajectory resulting from the descent-only strategy.
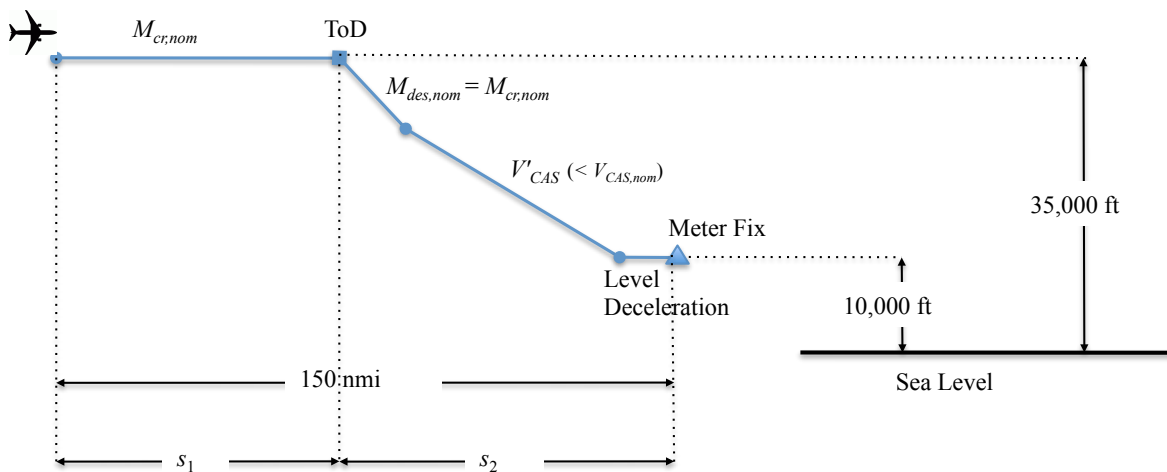

Figure 6. Vertical trajectory profile for the descent-only strategy.

C. Cruise-first Strategy

As the name suggests, the cruise-only strategy is employed first. This results in some amount of delay being absorbed. The remaining delay is absorbed by following the descent-only strategy. Transition from Mach to CAS occurs at the altitude where the reduced Mach obtained from the first step equals the reduced CAS obtained from the second step. Figure 7 depicts the conceptual trajectory resulting from the cruise-first strategy.
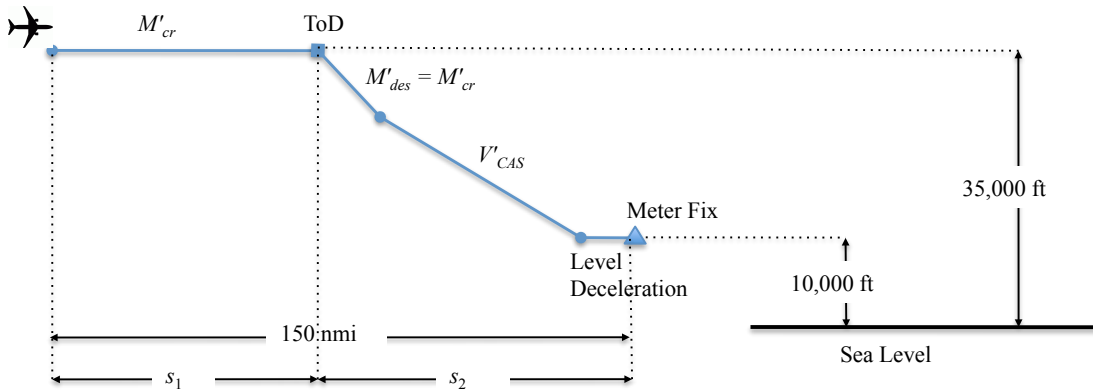

Figure 7. Vertical trajectory profile for the Cruise-first and Descent-first strategies.

D. Descent-first Strategy

This strategy also consists of the combination of descent-only and cruise-only strategies, except that descent-only strategy is employed first to absorb as much delay as possible and then the cruise-only strategy is employed to absorb the remaining delay. Thus, CAS is reduced first and then cruise Mach. Figure 7 also shows the trajectory resulting from this **strategy**.

E. Path stretch Strategy

When speed reduction is not sufficient to absorb the delay, a longer route can be flown to absorb the needed delay. Flying a longer route to absorb delay is known as the path stretch maneuver. An example of the resulting trajectory is shown in Fig. 8. In practice, air traffic controllers typically slow the aircraft down to cruise Mach $M_{cr,min}$ prior to vectoring the aircraft on a stretched path that terminates at the ToD point. After the ToD point, the aircraft descends at the reduced Mach until the desired CAS is captured, which can be equal to or less than $V_{CAS,nom}$. For

example, EDA issues advisories that have been computed using $V_{CAS,min}$. The total distance flown to the meter fix becomes greater than s_0 as a result of the path stretch.
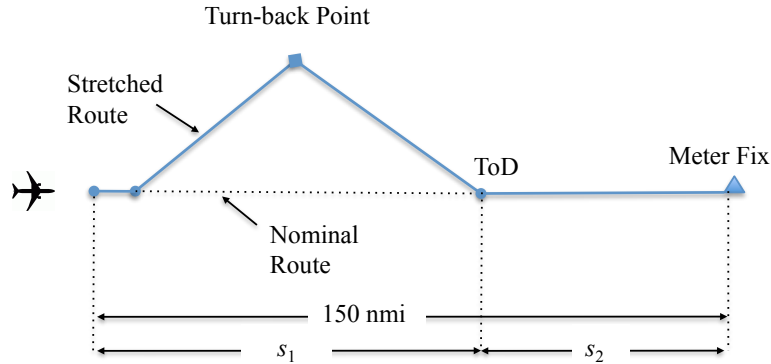

Figure 8. Lateral trajectory in path stretch. (plain view)

The unknown variable in this strategy is the length of the path stretch segment. The algorithm first estimates the length of the cruise and descent segments, s_1 and s_2, using the reduced Mach, and the nominal (or reduced) CAS without assuming path stretch. The resulting time of arrival at the meter fix is then subtracted from RTA. This time difference ΔT is then absorbed through path stretch. The length of the path stretch segment required for meeting RTA constraint at the meter fix is obtained by multiplying ΔT with $a \cdot M_{cr,min}$.

F. Intermediate Cruise Segment Strategy

In this strategy, a step-down descent is employed in which an Intermediate Cruise Segment (ICS) of length l_1 is specified at a pre-determined altitude h_1. While the total distance to the fix remains s_0, the length of the cruise segment is reduced by l_1 as illustrated in Fig. 9. The cruise segment is flown at $M_{cr,min}$. After the ToD point, descent is continued at $M_{cr,min}$ until the CAS becomes $V_{CAS,min}$. This segment is flown at a fixed flight path angle, which in this paper is assumed to be $\gamma = 3.14°$ or 1000 ft every 3 nautical miles. Thrust varies according to Eq. (21); it can be greater than idle-thrust. ICS is then flown at $V_{CAS,min}$ of the preceding descent segment. After the end of the ICS, descent to the meter fix is continued at the same CAS and at idle-thrust. The algorithm tries several ICS length values up to s_1, therefore $l_1 \leq s_1$, until a sufficiently large value is found that results in the time of arrival at the meter fix to be within ± 5 s of the RTA.
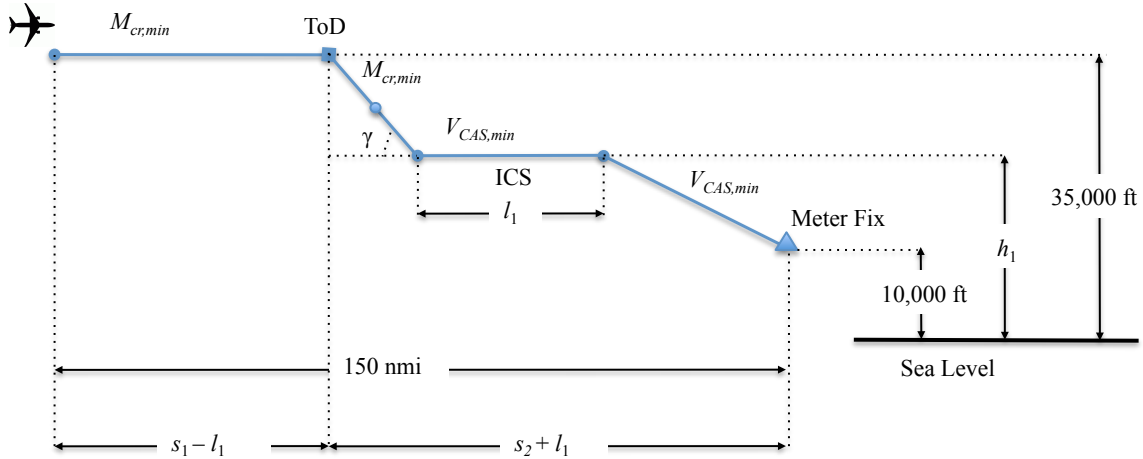
Figure 9. Illustration of a descent with intermediate cruise segment.

VI. Results

To ensure that conclusions hold for commercial jets, Boeing 737-800, 747-400, 757-300, 767-400, and 777-300, and Airbus A310-204, A320-231, A330-301, A340-642, and A380-841 models have been considered in this study. For ease of presentation, most of the results and observations in the subsequent sections are described with the Boeing 737-800 model. Results obtained with other aircraft models that were found to be qualitatively different than those obtained with the Boeing 737 model are also discussed.

Boeing 737-800 consumes 511 kg of fuel to fly its nominal trajectory from the TMA freeze horizon to the meter fix following the procedure described in section IV. Fuel burn estimates discussed below are with respect to this baseline value.

A. Speed Control Only

As discussed earlier in section V, cruise-only, descent-only, cruise-first and descent-first speed control strategies can be used to absorb delay for meeting the RTA. These strategies can be implemented using the following three sets of controls, 1) idle-thrust descent at constant Mach and after transition altitude at constant CAS, or simply called *constant Mach/CAS*, 2) fixed flight path angle descent at constant Mach/CAS, and 3) idle-thrust descent at fixed flight path angle. Results obtained with these three sets of controls are discussed below.

1. Idle-thrust Descent at Constant Mach/CAS

Descent at idle-thrust and constant Mach/CAS is the most common descent procedure employed by pilots of large jets equipped with an FMS capable of performance-based VNAV. Figure 10 shows the fuel consumption of Boeing 737-800, expressed as a percentage of the nominal fuel consumption of 511 kg, for absorbing different amounts of delay using the cruise-only, descent-only, cruise-first, and descent-first strategies. The descent portion of the trajectory in these four strategies is conducted at idle-thrust. Table 3 provides the needed Mach and CAS combinations. Observe in Figure 10 that the entire range of delays cannot be absorbed by all the strategies. For example, the cruise-only strategy and the descent-only strategy cannot be used to absorb delays greater than 70 s and 110 s, respectively, given a minimum Mach of 0.71 and a CAS of 250 knots. Cruise-first and descent-first strategies can be used to absorb larger delays. Note that the cruise-first results are identical to cruise-only results for delays up to 70 s and, therefore, the respective curves overlap in Fig. 10. Similarly, descent-first results are the same as descent-only results for delays up to 110 s. As expected, fuel consumption using descent-first is the same as that obtained using cruise-first for minimum Mach and CAS combination of 0.71 and 250 knots. This occurs at the 160 s delay location.
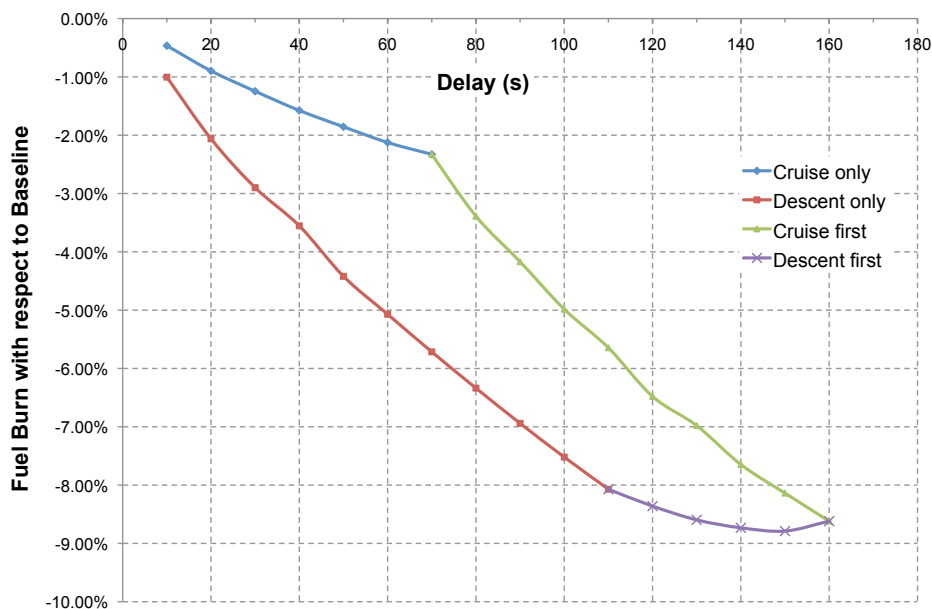

Figure 10. Fuel burn for Boeing 737-800 idle-thrust descent at constant Mach/CAS.

American Institute of Aeronautics and Astronautics

Table 3. Mach/CAS combinations to absorb delay for Boeing 737-800.

Delay (s)	Cruise-only	Descent-only	Cruise-first	Descent-first
10	0.77/290	0.78/285	0.77/290	0.78/285
20	0.76/290	0.78/280	0.76/290	0.78/280
30	0.75/290	0.78/276	0.75/290	0.78/276
40	0.74/290	0.78/273	0.74/290	0.78/273
50	0.73/290	0.78/269	0.73/290	0.78/269
60	0.72/290	0.78/266	0.72/290	0.78/266
70	0.71/290	0.78/263	0.71/290	0.78/263
80		0.78/260	0.71/283	0.78/260
90		0.78/257	0.71/278	0.78/257
100		0.78/254	0.71/273	0.78/254
110		0.78/251	0.71/269	0.78/251
120			0.71/264	0.77/250
130			0.71/261	0.76/250
140			0.71/257	0.74/250
150			0.71/254	0.73/250
160			0.71/251	0.71/251

The descent-first strategy is the most fuel-efficient strategy for the entire range of delays. Reducing descent CAS first results in more time spent in idle-thrust condition compared to reducing cruise Mach first, which results in more time spent at higher thrust. The descent-first strategy was found to be the most fuel efficient for all ten aircraft considered.

Moreover, the descent-only strategy results in trajectories with lower fuel burn than the nominal trajectory. As shown in Fig. 11, reducing the descent CAS results in a longer descent segment. ToD point is shifted further upstream and the length of the cruise segment is reduced from s_1 to s'_1. The aircraft spends more time on idle-thrust setting and less at higher cruise thrust compared to the nominal trajectory. This results in lower fuel consumption.
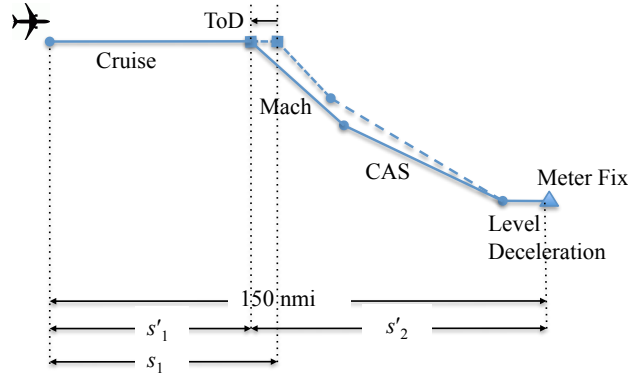
Figure 11. Shift of Top-of-Descent point due to reduced descent CAS.

Figure 12 shows the fuel consumption of a Boeing 757-300 as a function of the four speed reduction strategies for absorbing different amounts of delay. Compared to the fuel burn trends seen in Fig. 10, where speed reduction always resulted in lower fuel consumption compared to the nominal trajectory, Fig. 12 shows that fuel consumption is higher using cruise-only and cruise-first for delays less than 120 s. While speed reduction leads to lower fuel flow (see Eq. (10)), flight time increases to cover the same distance. The amount of fuel consumed depends on both the fuel flow and the flight time as shown in Eq. (13). For delays less than 120 s, the drop in B757-300 fuel flow due to reduced Mach was not large enough to offset the increase in flight time. Thus, fuel burn increased compared to the B757-300 nominal trajectory.
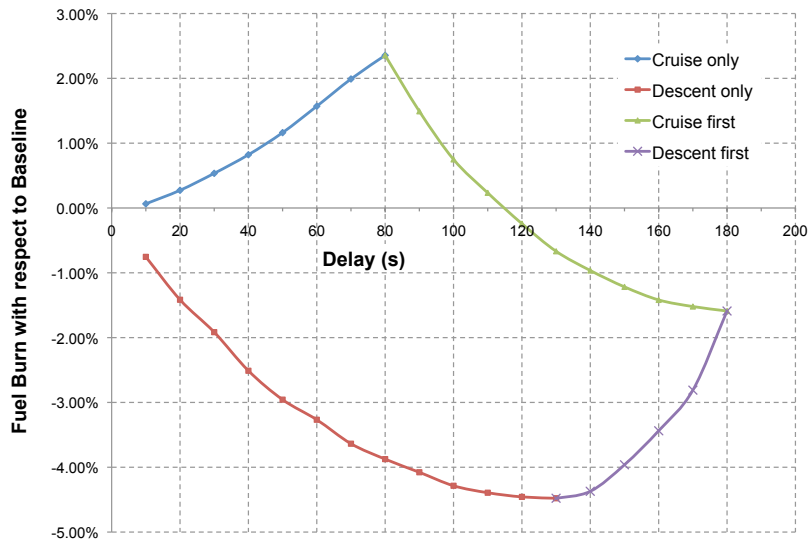

Figure 12. Fuel burn for Boeing 757-300 idle-thrust descent at constant Mach/CAS.

2. Constant Flight Path Angle Descent at Constant Mach/CAS

These types of descents are frequently executed by regional/business jets equipped with more limited FMS/VNAV capabilites. In large commercial jets, the pilot procedures for configuring the FMS to fly fixed-angle descents from TOD are often cumbersome, despite having more sophisticated VNAV capabilities.. In spite of this fact, constant flight path angle descent at constant Mach/CAS is examined for large commercial jets. It turns out that in many instances it yields lower fuel consumption than idle-thrust descent at constant Mach/CAS. Similar findings are reported in Ref. 14.

Figure 13 shows fuel consumption results for Boeing 737-800 obtained using cruise-only, descent-only, cruise-first and descent-first strategies with the procedure shown in Fig. 2. A fixed γ of 2.5 degrees, corresponding to a descent of 800 ft every 3 nmi, was used for generating these results. In some cases, $V_{CAS,min}$ was set higher than 250 kn to ensure that the required thrust to execute this procedure did not drop below idle-thrust. Deployment of speed brakes was not considered in this analysis.
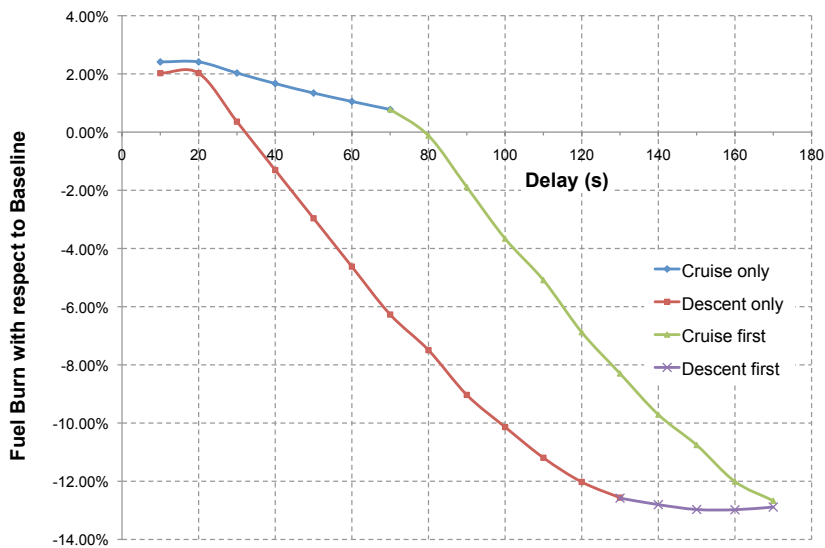

Figure 13. Additional fuel burn for Boeing 737-800 fixed flight path angle descent at constant Mach/CAS.

Comparing the descent-only curve in Fig. 13 to that in Fig. 10, it is seen that for delays greater than 70 s, descent at constant flight path angle results in lower fuel consumption. A similar comparison was performed for all other aircraft. Table 4 lists the preferred strategy that results in lower fuel consumption for each aircraft. That includes either idle-thrust descent at constant Mach/CAS (IT) or constant flight path angle descent at constant Mach/CAS (CFPA). For example, a B737 IT descent results in less fuel consumption for delays up to 70 s, while CFPA descent

results in lower fuel consumption for delays $\geq 70\,$s. The third column in the table lists the minimum and maximum percent difference in fuel burn between IT and CFPA for the entire range of delay values analyzed, computed by the following metric:

$$\frac{\left(CFPA \text{ fuel burn}\right) - \left(IT \text{ fuel burn}\right)}{\left(IT \text{ fuel burn}\right)} \cdot 100 \tag{23}$$

Table 4. Comparison between descents at idle-thrust and fixed flight path angle

Aircraft Type	Preferred Strategy	Range of % difference in fuel burn between IT and CFPA
B737	IT < 70 s; CFPA ≥ 70 s	[-5%, +3%]
B747	CFPA	[-8%, 0%]
B757	CFPA	[-6%, -3%]
B767	CFPA	[-5%, -2%]
B777	CFPA	[-5%, -1%]
A310	IT	[0%, +4%]
A320	IT	[+2%, +10%]
A330	IT	[+1%, +3%]
A340	IT	CFPA not feasible
A380	IT	CFPA not feasible

Thus for the B737 model, the percent difference in fuel burn as computed by Eq. (23) was found to range between -5% and +3% for delays ranging between $10\,$s and $160\,$s. It should be noted that IT and CFPA descents could not be compared for A340 and A380 because less than idle-thrust is needed with CFPA of 2.5 degrees for the chosen range of delays. Since thrust cannot be lowered below idle-thrust, the only way to conduct CFPA is by slowing down the aircraft, which would require deployment of speed brakes. This condition has not been examined in this study.

B. Path stretch

Path stretch is employed for absorbing large delays that cannot be absorbed solely by speed control, which is limited by minimum speed. Results were generated for the ten aircraft types by first reducing the cruise Mach to minimum Mach (0.71 for large aircraft and 0.74 for heavy aircraft), then conducting a path stretch at the reduced cruise Mach and subsequently descending at a constant CAS after the Mach transition altitude.

Figure 14 shows B737 fuel consumption when an aircraft executes a path stretch, as described in subsection V.E, and for values of descent CAS ranging between the nominal value of 290 kn and the lower value of 250 kn. As an example, the line corresponding to 270 kn shows that 240 s of delay can be absorbed by executing a path stretch and then descending at a CAS of 270 kn. Delay absorption of 240 s comes at the cost of 10% more fuel consumption compared to that consumed flying the nominal trajectory. This same amount of delay can also be absorbed by descending at the CAS of 250 kn with an increased fuel consumption of only +0.3% with respect to baseline usage flying the nominal trajectory. A strictly monotonic decrease in fuel consumption is observed with lower descent CAS. Observe that the data-point on the graph for CAS of 250 kn corresponding to delay of 160 s and fuel consumption of about -9% is the same as the one shown in Fig. 10 where the cruise-first and descent-first graphs meet. This condition corresponds to minimum cruise Mach of 0.71 and minimum descent CAS of 250 kn. The delay of 160 s is absorbed entirely by speed control, without path stretch. This means that speed control should be exhausted prior to initiating a path stretch to absorb delays. An extensive analysis on the optimum logic for switching from speed reduction to path stretch is included in Ref. 8. Similar conclusions were reached for the other nine aircraft considered in this study.
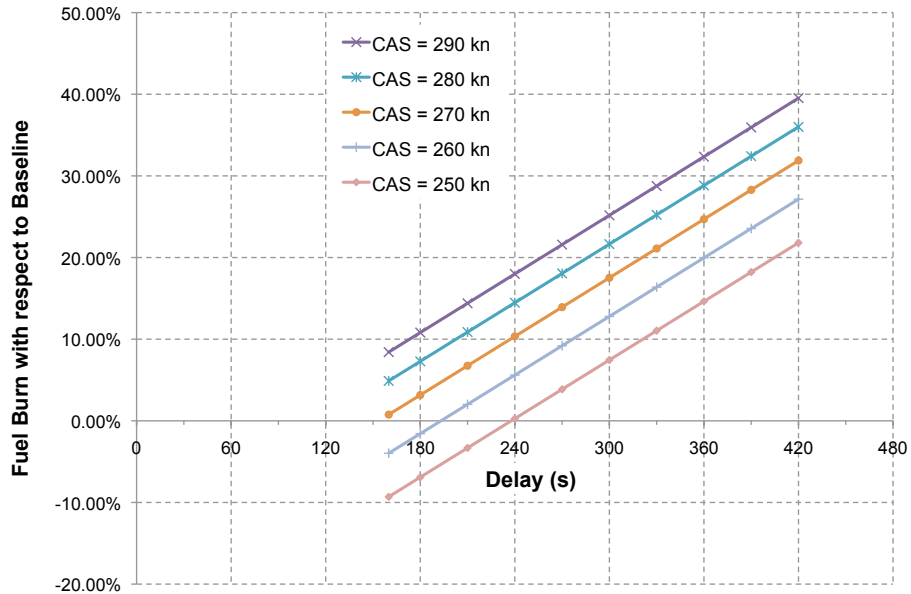

Figure 14. Fuel burn for Boeing 737-800 under path stretch with different descent CAS values.

C. Comparison between Path Stretch and Intermediate Cruise Segment

Next, the two most commonly used strategies for absorbing delays greater than three minutes are compared: 1) path stretch at high altitude, and 2) cruise at an intermediate altitude without path stretch. For the path stretch strategy, the aircraft is initially assumed to be at 35,000 ft and cruising at the reduced Mach of $M_{cr,min}$. Path stretch maneuver is done to absorb the assigned amount of delay till the aircraft reaches the ToD point. The aircraft then descends at constant $M_{cr,min}$ until it reaches the desired CAS. Descent is continued at this CAS all the way to 10,000 feet altitude.

Two CAS values, $V_{CAS,nom}$ and $V_{CAS,min}$, have been considered in this study. Descent at nominal CAS is frequently conducted in today's operations, while descent at minimum CAS is preferred by EDA for fuel efficient descent. Figure 15 shows B737 results with minimum CAS of 250 kn and nominal CAS of 290 kn. Figure 16 shows A340 results with minimum CAS of 250 kn and nominal CAS of 300 kn.
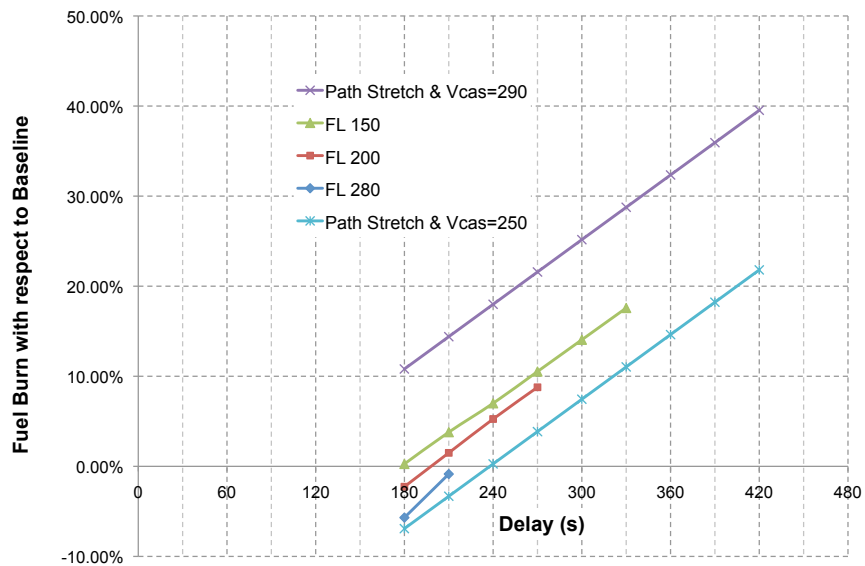

Figure 15. Additional fuel burn with respect to nominal trajectory for Boeing 737-800 path stretch with ICS.
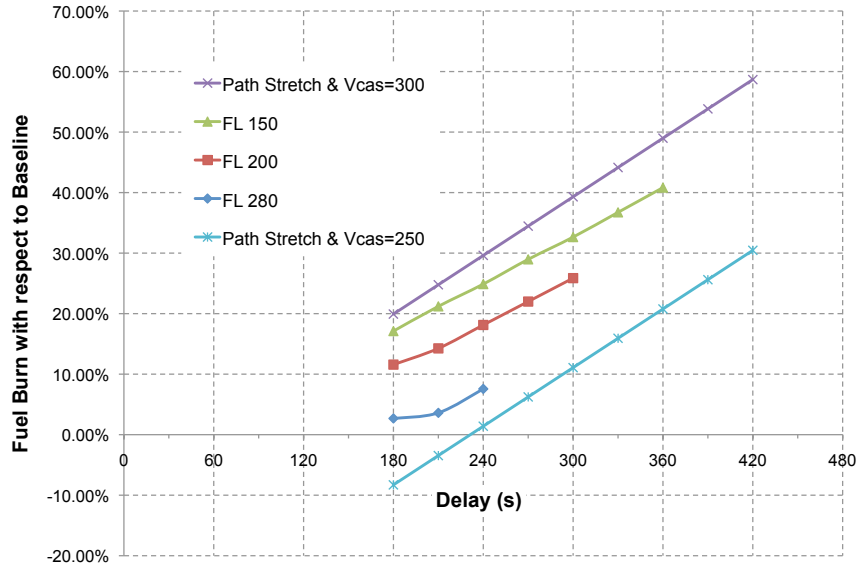
Figure 16. Additional fuel burn with respect to nominal trajectory for Airbus A340-642 path stretch with ICS.

Other graphs in Figs. 15 and 16 were generated using the Intermediate Cruise Segment maneuver, described in subsection V.F. Recall that the length of the intermediate cruise segment l_1 is a dependent variable in this maneuver; the length required for ensuring that the aircraft meets its RTA at the meter fix is determined. Figures 15 and 16 show results for delays ranging between 180 s and 420 s with intermediate cruise altitudes of 28,000 ft (FL 280), 20,000 ft (FL 200), and 15,000 ft (FL 150).

The graphs in both figures indicate that less fuel is required to execute a path stretch maneuver at 35,000 ft and descend at *minimum* CAS of 250 kn, which is the EDA strategy, compared to that using the ICS strategy. This finding, valid for all ten aircraft types considered in this study, is partly due to higher fuel flow rates when the aircraft is cruising at lower altitudes. However, it is more fuel-efficient to absorb delay using ICS at 15,000 ft compared to using path stretch at 35,000 ft with descent at *nominal* CAS for this range of delays. This is because the ICS strategy assumed minimum speed during descent to the meter fix (see Fig. 9), whereas path stretch assumed descent at nominal CAS. ICS is not feasible for all delay values. For example, A340 cannot absorb delays greater than 240 s with intermediate cruise at 28,000 ft because a length l_1 greater than the total distance to be covered, s_0, is required. The best strategy for absorbing the entire range of delays in Figs. 15 and 16 from a fuel usage perspective is to cruise at minimum speed, do a path stretch at high altitude at that minimum speed, and then descend at minimum speed.

VII.   Variations in Cruise Altitude and Wind

Analysis in the previous sections assumed cruise altitude of 35,000 ft and zero wind. In this section the impact of wind and of different cruise altitudes on fuel consumption is studied. The purpose is to examine whether the key finding of the case with zero wind and 35,000 ft cruise altitude, that the strategy which yields lower fuel consumption among alternative ones is first reduce descent CAS then cruise Mach and then execute a path stretch, is still valid for other cruise altitudes and when a wind scenario is taken into account.

Two additional cases with aircraft initially cruising at 33,000 ft and at 37,000 ft were considered. In this way, the effect of cruising altitude is covered for the typical range of cruise altitudes of commercial flights.

Moreover, the effect of wind velocity on the ranking of descent trajectories was also considered. Four additional cases were examined, two assuming headwind and two assuming tailwind blowing uniformly at a speed of 30 knots and 60 knots from cruise altitude to 10,000 ft. To account for wind, Eq. (3) is re-written as:

$$\dot{s} = V \cos \gamma + u_w \tag{24}$$

where u_w is the along-track component of wind velocity; it takes positive values for tailwind and negative for headwind.

For each combination of cruise altitude and wind speed, a set of delay values were again assigned to each aircraft type, to repeat the analysis discussed in Section VI. The following subsections present and discuss the findings of the analysis, organized by delay absorption strategy.

A. Idle-thrust Descent at Constant Mach/CAS

This subsection compares fuel consumption of cruise-first and descent-first strategies for descents at idle thrust and constant Mach/CAS. The analysis considered all combinations of cruise altitude and wind speed, including the baseline scenario of 35,000 ft cruise altitude and zero wind that was discussed in the previous section of the paper. For each combination and for each aircraft type, the strategy that resulted in lower fuel consumption was identified. Table 5 summarizes the findings: *Descent-first* is listed for scenarios where the descent-first strategy resulted in lower fuel consumption for all aircraft types..Otherwise, the particular aircraft types for which cruise-first resulted in lower fuel consumption are listed. As an example, for the scenario with 60 knots of headwind and cruise altitude at 35,000 ft, Descent-first was found to yield lower fuel consumption for all aircraft types except for the B737 and the A330 types, for which Cruise-first strategy resulted in lower fuel consumption.

Table 5. Comparison between Cruise-first and Descent-first procedures for different cruise altitudes and wind conditions. (aircraft type names are used when Cruise-first was more fuel efficient)

	33,000 ft	35,000 ft	37,000 ft
Zero wind	Descent-first	Descent-first	Descent-first
Headwind 30 knots	Descent-first	Descent-first	Descent-first
Headwind 60 knots	B737, A310, A330	B737, A330	A330
Tailwind 30 knots	Descent-first	Descent-first	Descent-first
Tailwind 60 knots	Descent-first	Descent-first	Descent-first

The results in Table 5 indicate that in the vast majority of cases, the *Descent-first* strategy is more fuel efficient than *Cruise-first* strategy. This finding is in accordance with the one analyzed in the previous section of this paper and it corresponds to the zero wind and 35000 ft cruise altitude case of Table 5. For those cases with a strong headwind of 60 knots, Descent-first is still more fuel efficient for most aircraft but not all. *Cruise-first* is more fuel-efficient for three aircraft types for cases where cruise altitude is 33000 ft. For cases with higher cruise altitude, *Cruise-first* is preferred for fewer aircraft types, two for 35000 ft and only one for 37000 ft. Therefore, first reducing speed during descent is more effective for cases where the descent phases is longer, as is the case when cruise altitude is at 37000 ft.

Descent-first results in lower fuel consumption in most of the cases examined. However, it turned out that Cruise-first is more fuel efficient for the popular B737 model in cases where there is a strong headwind and cruise altitude is 35000 ft or lower.

B. Comparison between Path Stretch and Intermediate Cruise Segment

Based on the findings for the case with zero wind and cruise altitude at 35,000 ft, presented in subsection VI.C, a path stretch maneuver with descent CAS at 250 knots was compared against descents that include an intermediate cruise segment, as described in subsection V.F. The analysis considered delays ranging between 180 s and 420 s with intermediate cruise altitudes of 28,000 ft, 20,000 ft, and 15,000 ft. For each combination of wind, initial cruise altitude, aircraft type, and delay assigned to that aircraft, path stretch with descent CAS 250 knots was compared to descent with intermediate cruise segment and the strategy that resulted in lower fuel consumption was identified. Table 6 summarizes the findings of the analysis.

It was found that in all cases the strategy of reducing cruise Mach to minimum possible followed by executing a path stretch maneuver and then descent at CAS of 250 knots yielded less fuel consumption that descents with

intermediate cruise segments. For instance, for initial cruise altitude of 33,000 ft and a uniform headwind of 60 knots, it was found that the path stretch strategy was more fuel efficient than the strategy with a level off segment – either at 28,000 ft or 20,000 ft or 15,000 ft, for all aircraft types and for all amounts of delay to be absorbed – ranging from 180 s to 420 s. The same result was found for all other combinations of wind and initial cruise altitude.

Table 6. Comparison between Path-stretch and Intermediate Level Segment procedures for different cruise altitudes and wind conditions.

	33,000 ft	35,000 ft	37,000 ft
Zero wind	Path-stretch & 250 CAS	Path-stretch & 250 CAS	Path-stretch & 250 CAS
Headwind 30 knots	Path-stretch & 250 CAS	Path-stretch & 250 CAS	Path-stretch & 250 CAS
Headwind 60 knots	Path-stretch & 250 CAS	Path-stretch & 250 CAS	Path-stretch & 250 CAS
Tailwind 30 knots	Path-stretch & 250 CAS	Path-stretch & 250 CAS	Path-stretch & 250 CAS
Tailwind 60 knots	Path-stretch & 250 CAS	Path-stretch & 250 CAS	Path-stretch & 250 CAS

To summarize the analysis presented in this section, three cases for initial cruise altitude – 33,000 ft, 35,000 ft, and 37,000 ft – and five cases for wind condition – zero wind, uniform headwinds of 30 knots and 60 knots, and uniform tailwinds of 30 and 60 knots – were examined. Since 10 aircraft types were considered, a total of 150 cases were analyzed. It was found that the most fuel efficient strategy to absorb delays that range from 10 s to 420 s is to plan for reducing first descent CAS as much possible, then reduce cruise Mach as much as possible, and then execute a path stretch maneuver at cruise altitude to absorb the remaining delay. A few exceptions to this rule were found, in particular 6 cases, all of which for headwind of 60 knots. When compared to the total 150 cases analyzed, in only 4 percent of the cases the previously-stated rule did not apply.

VIII.   Conclusions

Fuel consumption of standard descent strategies from cruise altitude to meter fix altitude with required time of arrival constraint specified at the meter fix were examined for five Boeing and five Airbus commercial jet aircraft using a point-mass equations of motion model and the Base of Aircraft Data (BADA) model. Four speed control techniques were considered for absorbing the delays needed for meeting the required time of arrival constraint at the meter fix with idle-thrust descent at constant Mach/calibrated-airspeed, namely cruise-only, descent-only, cruise-first and descent-first. Of these four techniques, the descent-first strategy, in which the descent calibrated-airspeed is reduced first to absorb as much delay as possible and then cruise Mach is reduced to absorb the remaining delay, turned out to be the most fuel efficient strategy for a wide range of delays.

Furthermore, comparison of 1) path stretch at high altitude and 2) descent without path stretch that includes cruise at an intermediate altitude led to the conclusion that the best approach from fuel consumption perspective is to cruise at minimum speed, complete a path stretch at high altitude at that minimum speed, and then descend at minimum speed. This strategy, together with the descent-first strategy, is used in the Efficient Descent Advisor to generate advisories for meeting the required time of arrival at the meter fix. The results of this paper helped to verify that EDA's delay-absorption strategies lead to minimum fuel burn. As such, the results of this paper helped to strengthen the case for transferring EDA to the FAA for eventual field deployment.

Combining the two major conclusions, it was found that the most fuel efficient strategy to absorb delays that range from 10 s to 420 s is to plan for reducing first descent CAS as much possible, then reduce cruise Mach as much as possible, and then execute a path stretch maneuver at cruise altitude. This result was verified through simulations for a wide range of cruise altitude and wind conditions. A few exceptions were found in which the Cruise-first strategy was favored.

The constant flight path angle descent at constant Mach/calibrated-airspeed, a procedure used by regional and business jets but not by large jets, was found to be more fuel efficient strategy compared to the standard descent at idle-thrust and at constant Mach/calibrated-airspeed in certain cases. For a scenario with zero wind and initial cruise altitude of 35,000 ft, the difference in fuel consumption with these two strategies ranged between -8% and +10%.

While this paper offers strong indications on the fuel efficiency of delay-absorbing strategies through simulations that use a point-mass equations of motion model, this work can continue in two fronts: a) derivation of the similar conclusions by means of mathematical proofs, and b) validation of the simulation results with actual flight data.

Acknowledgments

References

[1] Swenson, H. N., Hoang T., Engelland S., Vincent D., Sanders T., Sanford B., and Heere K., "Design and Operational Evaluation of the Traffic Management Advisor at the Fort Worth Air Route Traffic Control Center," *1ˢᵗ USA/Europe Air Traffic Management Research and Development Seminar*, Online Proceedings, 1997.

[2] Coppenbarger, R., Lanier, R., Sweet, D., and Dorsky, S., "Design and Development of the En Route Descent Advisor (EDA) for Conflict-Free Arrival Metering," *AIAA Guidance, Navigation, and Control Conference and Exhibit*, Online Proceedings, AIAA, Reston, VA, 2004.

[3] Mueller, K. T., Bortins, R., Schleicher, D., Sweet, D., and Coppenbarger, R., "Effect of Uncertainty on En Route Descent Advisor (EDA) Predictions," *AIAA Aviation Technology, Integration and Operations Conference*, Online Proceedings, AIAA, Reston, VA, 2004.

[4] Coppenbarger, R., Dyer, G., Hayashi, M., Lanier, R., Stell, L., and Sweet, D., "Development and Testing of Automation for Efficient Arrivals in Constrained Airspace," *27ᵗʰ Congress of the International Council of the Aeronautical Sciences*, Online Proceedings, ICAS Secretariat, Bonn, Germany, 2010.

[5] Coppenbarger, R., Mead, R., and Sweet, D., "Field Evaluation of the Tailored Arrivals Concept for Datalink-Enabled Continuous Descent Approach," *Journal of Aircraft*, Vol. 46, No. 4, 2009, pp. 1200-1209.

[6] Shresta, S., Neskovic, D., and Williams, S. S., "Analysis of Continuous Descent Benefits and Impacts During Daytime Operations," *8ᵗʰ USA/Europe Air Traffic Management Research and Development Seminar*, Online Proceedings, 2009.

[7] Robinson, III, J. E., and Kamgarpour, M., "Benefits of Continuous Descent Operations in High-Density Terminal Airspace Under Scheduling Constraints," *AIAA Aviation Technology, Integration, and Operations Conference*, Online Proceedings, AIAA, Reston, VA, 2010.

[8] Erzberger, H., "Automation of On-Board Flight Management," *Collection of papers of the 24ᵗʰ Israel Annual Conference on Aviation and Astronautics*, Israel, 1982, pp. 1-19.

[9] Sorensen, J. A., and Waters, M. H., "Airborne Method to Minimize Fuel with Fixed Time-of-Arrival Constraints," *Journal of Guidance and Control,* Vol. 4, No. 3, 1981, pp. 348-349.

[10] Franco, A., Rivas, D., and Valenzuela, A., "Minimum-Fuel Cruise at Constant Altitude with Fixed Arrival Time," *Journal of Guidance, Control, and Dynamics*, Vol. 33, No. 1, 2010, pp. 280-285.

[11] "User Manual for the Base of Aircraft Data (BADA) Revision 3.9," Eec note no. 11/08, Eurocontrol Experimental Centre, Nov. 2008.

[12] Slattery, R., and Zhao, Y., "Trajectory synthesis for air traffic automation," *Journal of Guidance, Control, and Dynamics*, Vol. 20, No. 2, 1997, pp. 232-238.

[13] Erzberger, H., and Tobias, L., "A time-based concept for terminal-area traffic management," NASA TM-88243, 1986.

[14] Wu, M., and Green, S., "Analysis of Fixed Flight Path Angle Descents for the Efficient Descent Advisor," *AIAA Guidance, Navigation, and Control Conference*, Online Proceedings, AIAA, Reston, VA, 2012.